CHAPTER 7

DESIGN AND DEVELOPMENT OF CYLINDRICAL DIELECTRIC RESONATOR ANTENNA USING BB GLASS ADDED BST (BST-3B) EXCITED BY NOVEL COMPOSITE FEED

7.1 Introduction

Dielectric resonator antenna (DRA) has attracted great attention in the research area since last three decades after the pioneering work done by Long et al. (1983). They first proposed an open dielectric resonator of cylindrical shape as an antenna in 1983. Since then different shapes of DRA, such as cylindrical, rectangular, triangular, hemispherical have been widely investigated.

Material selection plays a crucial role in determining the final performance of an antenna or any other device. The antenna engineers constantly demand high quality ceramic materials to design their microwave modules or antennas. Materials should fulfil the primary need of good microwave dielectric properties along with low processing and fabrication cost. Barium Strontium Titanate (BST) is widely used for microwave applications because of its good properties of high permittivity, low loss tangent, better thermal and mechanical responses, and good tunability [Lekshmi et al. (2018); Coronado et al. (2014); Brankovic et al. (2005)]. But due to its high sintering temperature, it is costly to manufacture. Liquid phase sintering is mostly preferred because of its cost effectiveness and ease of synthesis [Li et al. (2016)].

To achieve monopole like radiation pattern, different multi-element DRAs have been widely investigated and reported in the literature [Guha et al. (2006b); Chaudhary et al. (2012); Gangwar et al. (2017); Kumari et al. (2018b)]. These DRAs show more complexity in their design and fabrication, which is not desirable at the medium or pilot scale production due to high manufacturing cost and time involved. Therefore, in the present study, more emphasis is given on the design of DRAs with simpler structure, for obtaining monopole like radiation pattern.

In the present investigation, 3 wt% BB glass added BST ceramic, named as BST-3B is used as dielectric resonator in the proposed single segment cylindrical DRA (SS-CDRA). The synthesis and characterization of BST-3B ceramic is described thoroughly in chapters 3 and 6, respectively. A new simple composite feeding technique consisting of a probe connected to XOR-shaped patch (PXP feed) is proposed to obtain the monopole like radiation pattern from SS-CDRA. The simulation and experimental studies on the proposed antenna were performed in microwave frequency range and results obtained for the antenna characteristics are compared. Simulation study on the antenna was carried out using Ansys HFSS software.

7.2 Antenna Design and Discussion

A single segment CDRA (SS-CDRA) is designed using Ansys High Frequency Structure Simulator (HFSS) simulation software. Three different feeding configurations (Figure 7.2) i.e. PPP [probe connected to plus-shaped patch], PSP [probe connected to swastika-shaped patch] and PXP [probe connected to XOR-shaped patch] are used for excitation of CDRAs of same dimensions and material constants. The parametric study is performed and the geometrical antenna parameters are optimized. The -10 dB reflection coefficient bandwidths for all the three CDRA-feed combinations show that the CDRA excited by feed 3 (PXP) provides the widest operating bandwidth among the three CDRA-feed combinations. The mode analysis for CDRA excited by feed 3 (PXP) reveals that it can provide monopole like radiation pattern over the operating bandwidth. Figure 7.1 shows the geometrical representation of the proposed antenna excited by PXP feed. Table 7.1 shows the optimized parameter values of the proposed antenna.

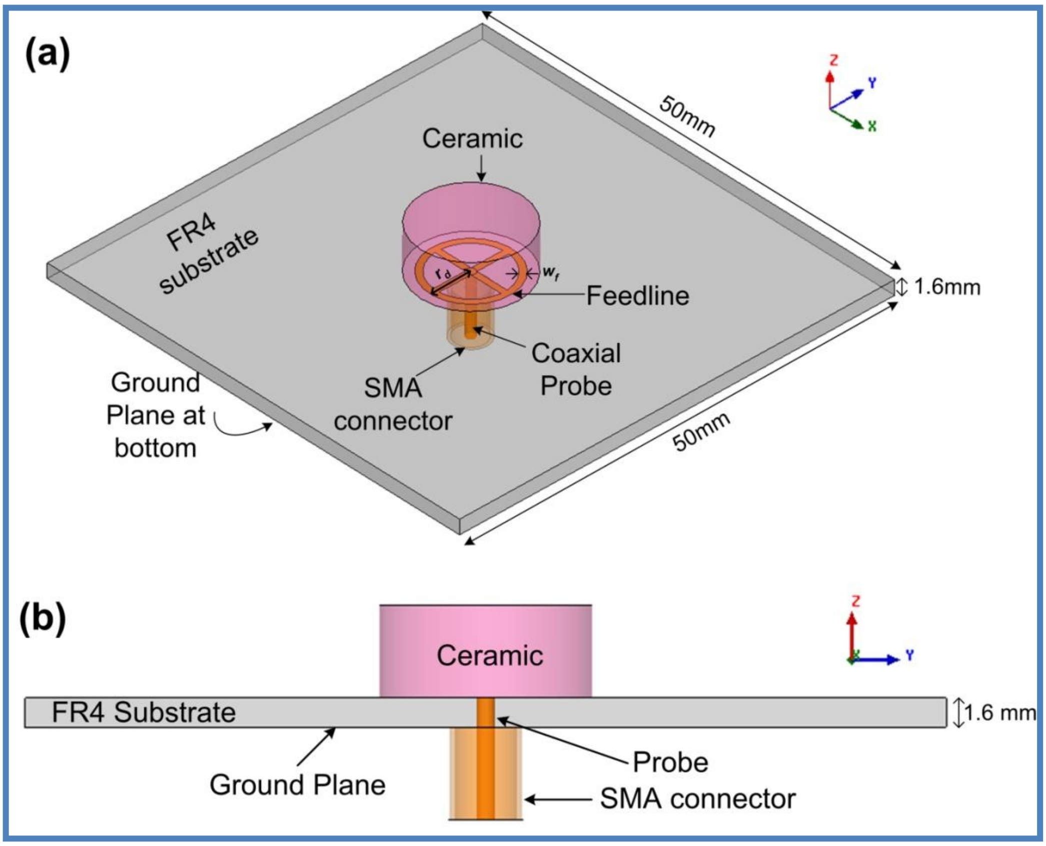

Figure 7.1 Geometry of proposed antenna (a) 3-D view (b) Side view

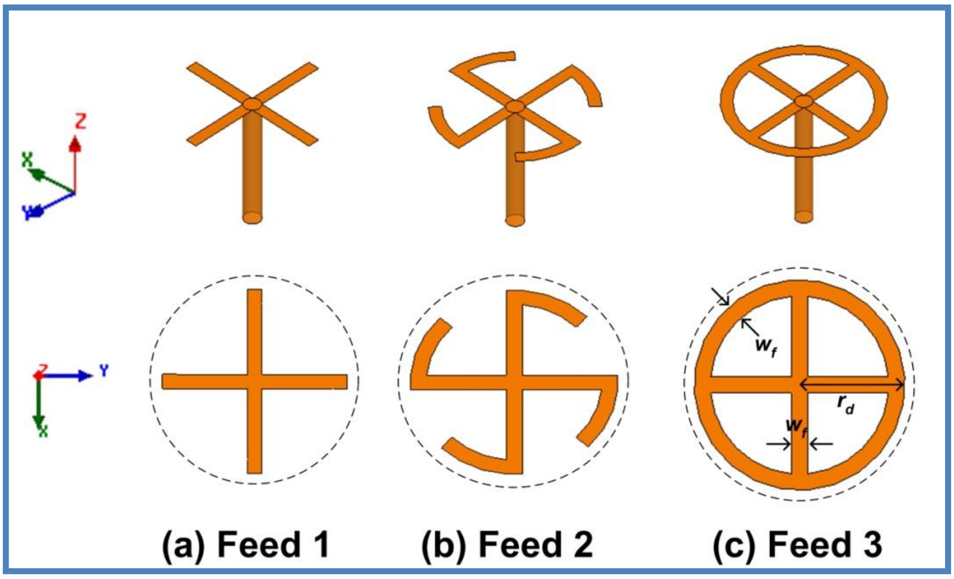

Figure 7.2 Different feed configurations for CDRA (a) Feed 1 (PPP), (b) Feed 2 (PSP), and (c) Feed 3 (PXP)

Table 7.1 Optimized design parameters of proposed CDRA.

Optimized parameters	**Dimensions**	**Materials**
Substrate dimension	50 mm × 50 mm × 1.6mm	FR4 (ε_r = 4.4)
Ground plane dimension	50 mm × 50 mm × 0.035 mm	Copper
Diameter (d_C) and Height(h_C) of CDRA	d_C = 11.5 mm, h_C = 5.0 mm	BST-B3 (ε_r = 17)
Width of printed patch, w_f	0.7 mm	Copper
Radius of outer periphery of ring of printed patch, r_d	4.7 mm	
Probe radius, r_p	0.5 mm	Copper
Feed position	Centre of the substrate/ground	-

The simulation study for the three CDRA-feed combinations was performed. Their reflection coefficient-frequency characteristics are shown in figure 7.3. The resonating frequency and -10 dB reflection coefficient bandwidth for the three CDRA-feed combinations are derived from figure 7.3 and the results are given in Table 7.2. It is observed from Table 7.2 that when CDRA is excited by feed 1 (PPP), negligible bandwidth (1.69 %) is obtained with resonating frequency of 12.38 GHz. This may be due to the fact that resonant element is getting negligible time to interact with the E field in the printed patch and the signal is lost from the edges of the printed patch (or the incident signal from the centre of the probe and the reflected signal from the edges of the printed patch are out of phase and thereby, cancel each other resulting in low E-field intensity and negligible coupling to the DR). In case of CDRA excited by feed 2 (PSP configuration), the E-field lines get enough time to interact with the DR while traversing through the swastika printed patch. Therefore, the CDRA fed through feed 2 configuration provides -10 dB reflection coefficient bandwidth of nearly 24 %, while its resonating frequencies are 7.7 and 8.9 GHz.

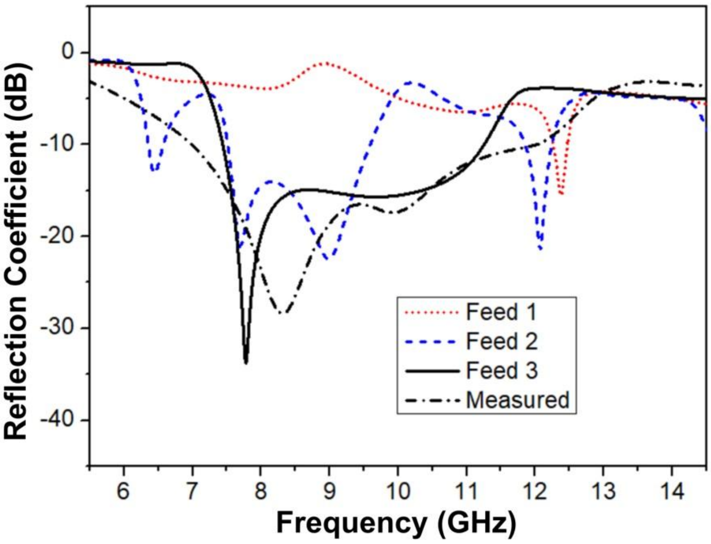

Figure 7.3 Simulated reflection coefficient-frequency characteristics of CDRA excited by three different feed configurations

Table 7.2 -10 dB reflection coefficient bandwidth and resonating frequency of the antenna for different feed configurations [Figure 7.3]

Type of Feed	Operating Bandwidth (GHz)	Resonating Frequency (GHz)	-10 dB Reflection Coefficient Bandwidth (%)
Feed 1(PPP)	12.26 - 12.47	12.38	1.69
Feed 2(PSP)	7.51 - 9.59	7.7, 8.98	24.33
Feed 3(PXP) (Proposed)	7.44 – 11.25	7.78	40.77

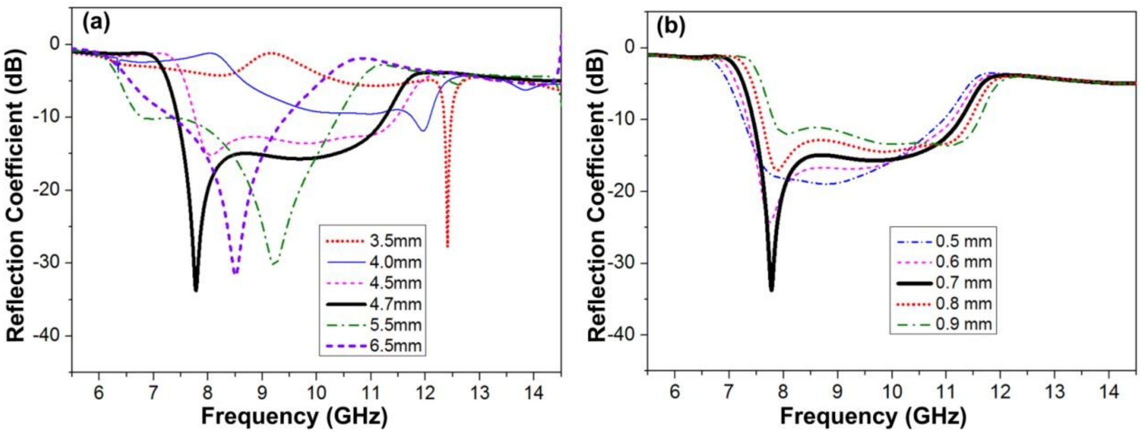

Figure 7.4 Simulated reflection coefficient-frequency characteristics of the proposed CDRA excited by feed 3 (a) for different 'r_d' values by keeping w_f =0.7 mm and (b) for different 'w_f' values by keeping r_d = 4.7 mm.

Table 7.3 -10 dB reflection coefficient bandwidth and resonating frequency of the antenna for different r_d values [Figure 7.4 (a)]

r_d (mm)	Operating Bandwidth (GHz)	Resonating Frequency (GHz)	Bandwidth (%)
3.5	12.34 - 12.48	12.41	1.13
4.0	11.76 - 12.08	11.96	2.68
4.5	7.76 - 11.47	-	38.58
4.7	7.44 - 11.25	7.78	40.77 (Proposed)
5.5	6.82 - 10.39	9.23	41.48
6.5	7.35 - 9.43	8.51	24.79

Table 7.4 -10 dB reflection coefficient bandwidth and resonating frequency of the antenna for different 'w_f' values by keeping r_d = 4.7 mm [Figure 7.4 (b)]

w_f (mm)	Operating Bandwidth (GHz)	Resonant frequency (f_o) in GHz	Bandwidth (%)
0.5	7.26 – 10.94	~8.05	40.43
0.6	7.34 – 11.11	7.74	40.86
0.7	7.44 – 11.25	7.78	40.77 (Proposed)
0.8	7.60 – 11.43	7.88	40.25
0.9	7.81 – 11.60	-	39.05

In the CDRA excited by feed 3 (PXP), the in-phase addition of E-field intensities takes place. The field intensity is less at four nodes (Node is the region where the plus-shape touches the circular ring of the printed patch) while the field intensity is maximum in regions other than node regions. Thus, wide -10 dB reflection coefficient bandwidth (40.77%) of the CDRA excited by feed 3 is obtained. Therefore, CDRA fed through feed 3 (PXP configuration) is chosen for further investigation.

The dimensions of the printed patch of feed 3 are optimized through simulation study. For parametric optimization, initially the outer radius (r_d) of the circular ring of printed patch in feed 3 is varied from 3.5 mm to 6.5 mm by keeping the printed patch width (w_f) constant at 0.7 mm. Figure 7.4 (a) shows the variations of reflection coefficient of CDRA excited by feed 3 versus frequency for different r_d values. Table 7.3 shows the values of resonating frequency and -10 dB reflection coefficient bandwidth for different r_d values. The widest bandwidth of 41.48 % (6.82-10.39 GHz) is obtained for r_d = 5.5 mm, but at lower frequencies in the range 6.82-7.50 GHz, the minimum reflection coefficient values lie near -10 dB. So that effective bandwidth of 7.5 - 10.39 GHz (32.31%) is considered for r_d = 5.5 mm. Therefore, optimized 'r_d' value of 4.7 mm is chosen which provides -10 dB reflection coefficient bandwidth of 40.77% (7.44-11.25 GHz). Now at this optimized r_d value, the parametric study is done by varying the printed patch width 'w_f' from 0.5 mm to 0.9 mm. The reflection coefficient-frequency characteristics of CDRA excited by feed 3 for different w_f values are shown in figure 7.4 (b) and the results are given in Table 7.4. The widest bandwidth of 40.86 % is obtained for w_f value of 0.6 mm. But when the graph given in figure 7.4 (b) is observed, the minimum reflection coefficient value of -33 dB is observed for the case of w_f = 0.7 mm at the resonant frequency of 7.78 GHz with sharp valley for which -10 dB reflection coefficient bandwidth of 40.77 % is obtained. Since 40.77 % bandwidth obtained for w_f = 0.7 mm is close to the bandwidth of 40.86 % achieved for w_f = 0.6 mm. Therefore, optimized value of w_f is chosen to be 0.7 mm for the proposed design.

Thus, the proposed antenna is fabricated as shown in figure 7.5 and its optimized dimensions are given in Table 7.1. The experimental as well as simulation studies on the proposed antenna were carried out. The experimental results are compared with the respective simulated ones.

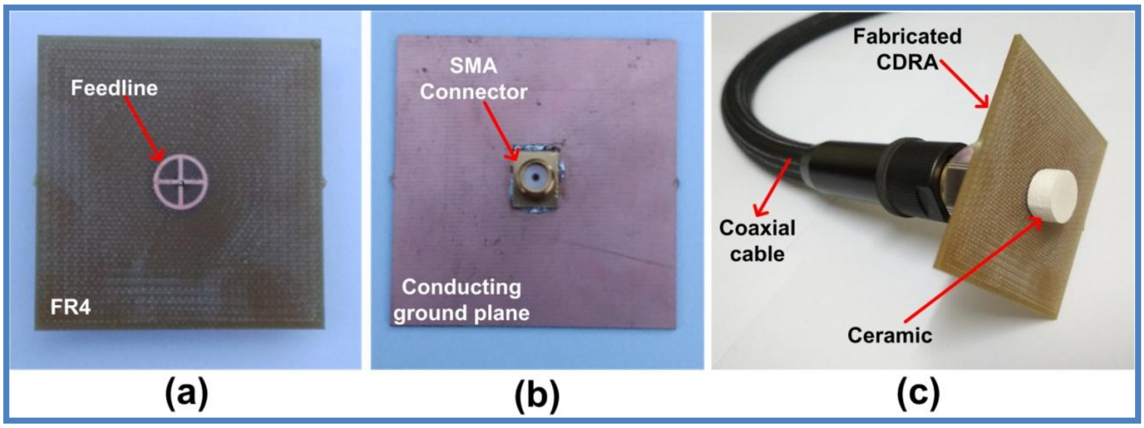

Figure 7.5 Image of fabricated antenna (a) Front side showing XOR patch (b) Bottom side (c) Image of the fabricated CDRA

7.3 Results and Discussion

7.3.1 Reflection coefficient – frequency characteristics

Measurement of reflection coefficient-frequency characteristics of the proposed antenna was made using Keysight make ENA E5071C network analyser**.** The experimental and simulated reflection coefficient-frequency characteristics of the proposed antenna is plotted in figure 7.6. It can be seen from figure 7.6 that experimental -10 dB reflection coefficient bandwidth and resonating frequency of the proposed antenna are found to be 52.08 % (7.03 - 11.98 GHz) and 8.30 GHz respectively, whereas respective simulated values are 40.77 % (7.44 - 11.25 GHz) and 7.78 GHz. The deviation in experimental and simulation results may have been caused due to fabrication and measurement errors.

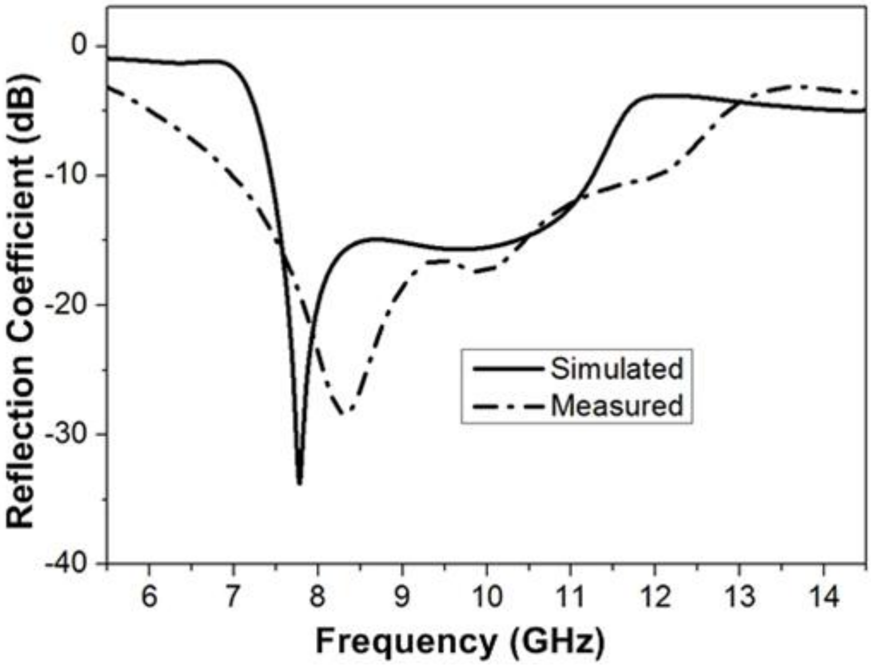

Figure 7.6 Reflection coefficient – frequency characteristics of the proposed antenna

7.3.2 Mode analysis

Figures 7.7 and 7.9 (a), (b) and (c) show E-field distributions in the printed patch and within CDR (cylindrical dielectric resonator) respectively at 12.38, 7.7 and 7.78 GHz. It is observed from figures 7.7 and 7.9 that the mode excited in the CDRA fed by PPP, PSP and PXP feeds are $TM_{01\delta}$, $TE_{01\delta}$ and distorted $TM_{01\delta}$ respectively.

The formula of theoretical resonant frequency (f_o) for the $TM_{01\delta}$ mode generated in isolated CDRA is given by:

$$f_o = \frac{c}{2\pi a(\sqrt{\varepsilon_r + 2})}\sqrt{(3.83)^2 + (\frac{a\pi}{2h})^2} \quad (7.1)$$

where ε_r is the dielectric constant of the CDRA material, *a* and *h* are radius and height of CDRA respectively, and *c* is speed of light in vacuum [Petosa (2007)]. The theoretical resonant frequency (f_o) for the proposed CDRA fed by PXP feed which excites distorted $TM_{01\delta}$ is estimated using equation (7.1).The theoretical resonant frequency of 8.06 GHz is obtained for proposed CDRA excited by PXP feed, whereas simulated resonant frequency is found to be 7.78 GHz (Table 7.4). The deviation between simulation and theoretical resonant frequencies may be due to the presence of higher order modes to some extent in the proposed antenna in addition to $TM_{01\delta}$ mode.

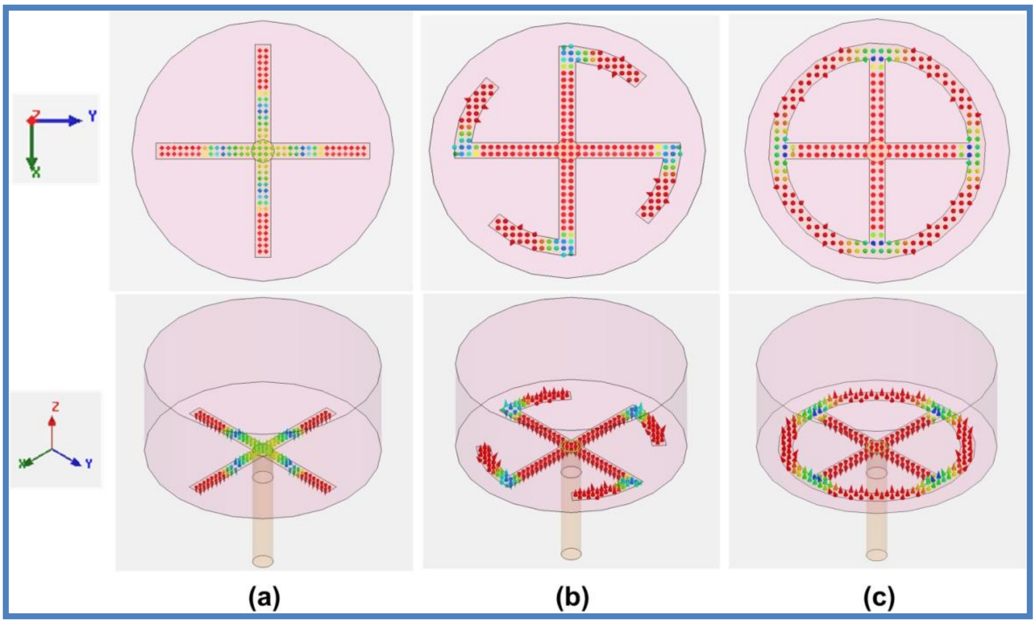

Figure 7.7 The E field distributions in the printed patches at their resonant frequencies for (a) Feed 1 (b) Feed 2 (c) Feed 3

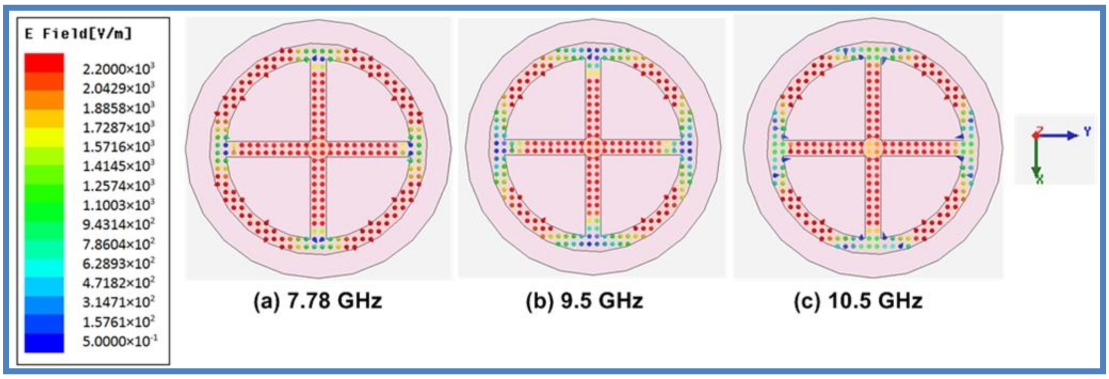

Figure 7.8 The E field distributions in the printed patch of proposed antenna at (a) 7.78 GHz (b) 9.5 GHz (c) 10.5 GHz.

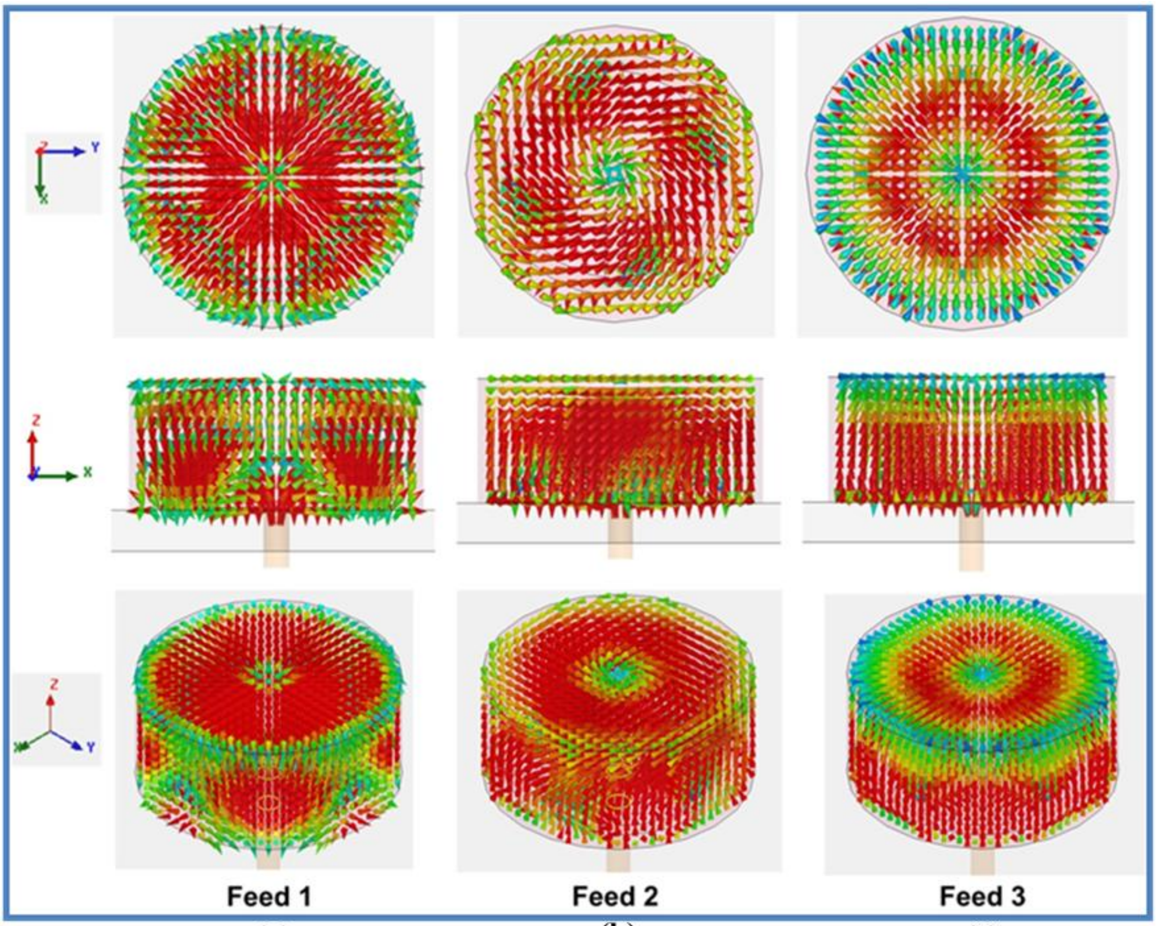

(a) (b) (c)

Figure 7.9 The E field distributions in the CDRA at corresponding resonant frequency for (a) Feed 1 (b) Feed 2 (c) Feed 3.

In the proposed CDRA excited by PXP feed (Feed 3), the E-field distribution is uniform in the plus-shaped feed as shown in figures 7.7 and 7.8. Figure 7.8 shows the E-field distribution in the printed patch of the proposed antenna at 7.78 GHz, 9.5 GHz and 10.5 GHz respectively. It is observed from figure 7.8 that the summation and cancellation of E-field components take place in the circular ring patch. At the nodes, the out of phase E-field components cancel each other, thus no E-field component is observed at the nodes, whereas in the remaining portion of the circular ring patch, the summation of in-phase E-field components takes place. Thus, overall E-field is enhanced in this region, which results in the wide operating bandwidth of 40.77 %.

7.3.3 Radiation patterns and gain of the proposed antenna

The simulation and measurement of radiation patterns of the proposed antenna at different frequencies were made. The radiation patterns at different frequencies within the operating frequency band were measured. The experimental and simulated radiation patterns in x-z, y-z and x-y planes at the frequencies of 7.44, 7.78, 8.3, 9.5, 10.5 and 11.25 GHz are shown in figures 7.10 and 7.11. The experimental patterns are found to be in agreement with the corresponding simulated patterns. The radiation patterns in x-y plane show some distortion with higher cross polarisation levels. Due to the existence of distorted $TM_{01\delta}$ mode, monopole like radiation pattern at any frequency of interest gets distorted. The higher cross polarisation level may be due to the presence of finite ground plane, type of feed and/or the radiation from the feed, and generation of the higher order modes. The 2D radiation patterns and 3D gain plots (Figure 7.12) of the proposed antenna show near to monopole like radiation characteristics up to the frequency of 10.5 GHz in its operating frequency range due to the aforesaid reasons. But the distorted patterns in x-y plane, though not exactly circular can still accommodate major area of interest. Distortion in radiation pattern and 3D gain plots are observed at higher frequencies which may be due to the diffraction from the edges of the antenna. The simulated and measured gain values of the proposed antenna were found to be 3.34 dB and 3.30 dB at their resonant frequencies of 7.78 GHz and 8.3 GHz, respectively.

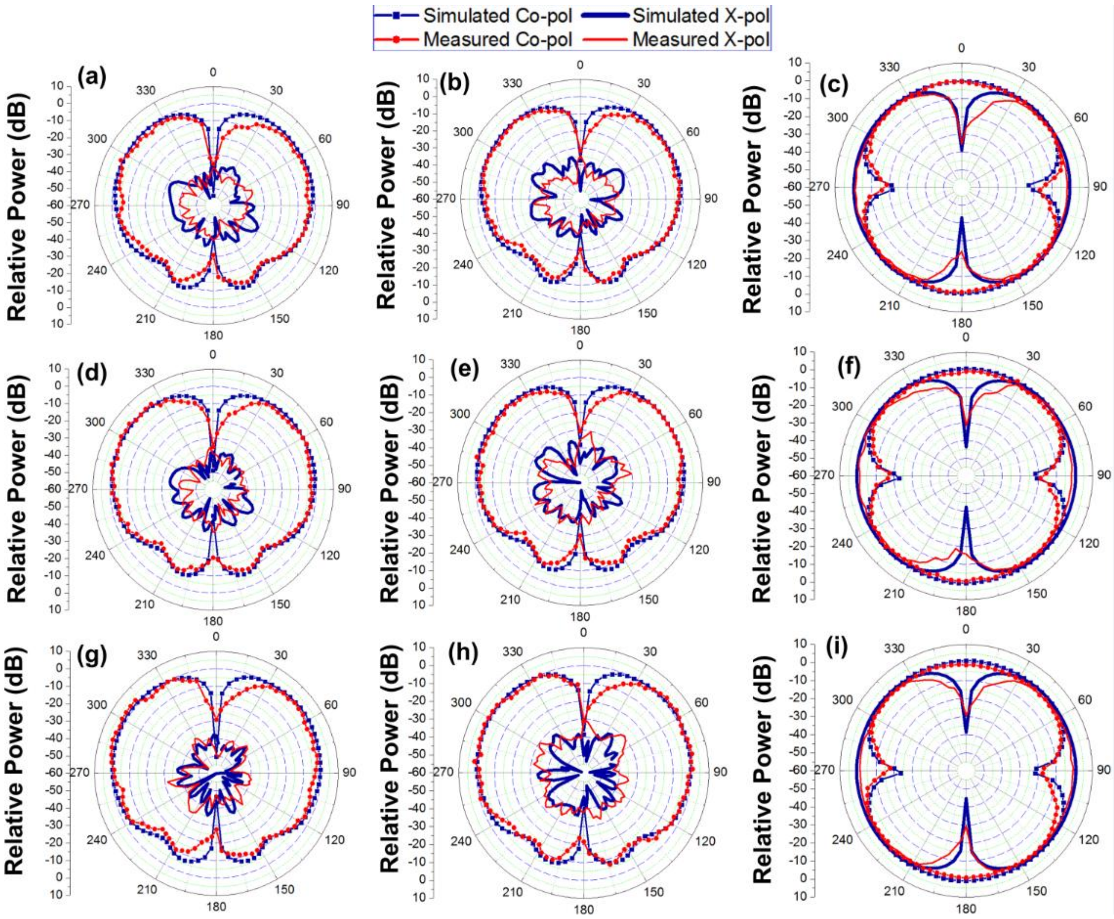

Figure 7.10 Radiation patterns of the proposed CDRA at (a) 7.44 GHz (in x-z plane); (b) 7.44 GHz (in y-z plane); (c) 7.44 GHz (in x-y plane); (d) 7.78 GHz (in x-z plane); (e) 7.78 GHz (in y-z plane); (f) 7.78 GHz (in x-y plane); (g) 8.30 GHz (in x-z plane); (h) 8.30 GHz (in y-z plane) and (i) 8.30 GHz (in x-y plane).

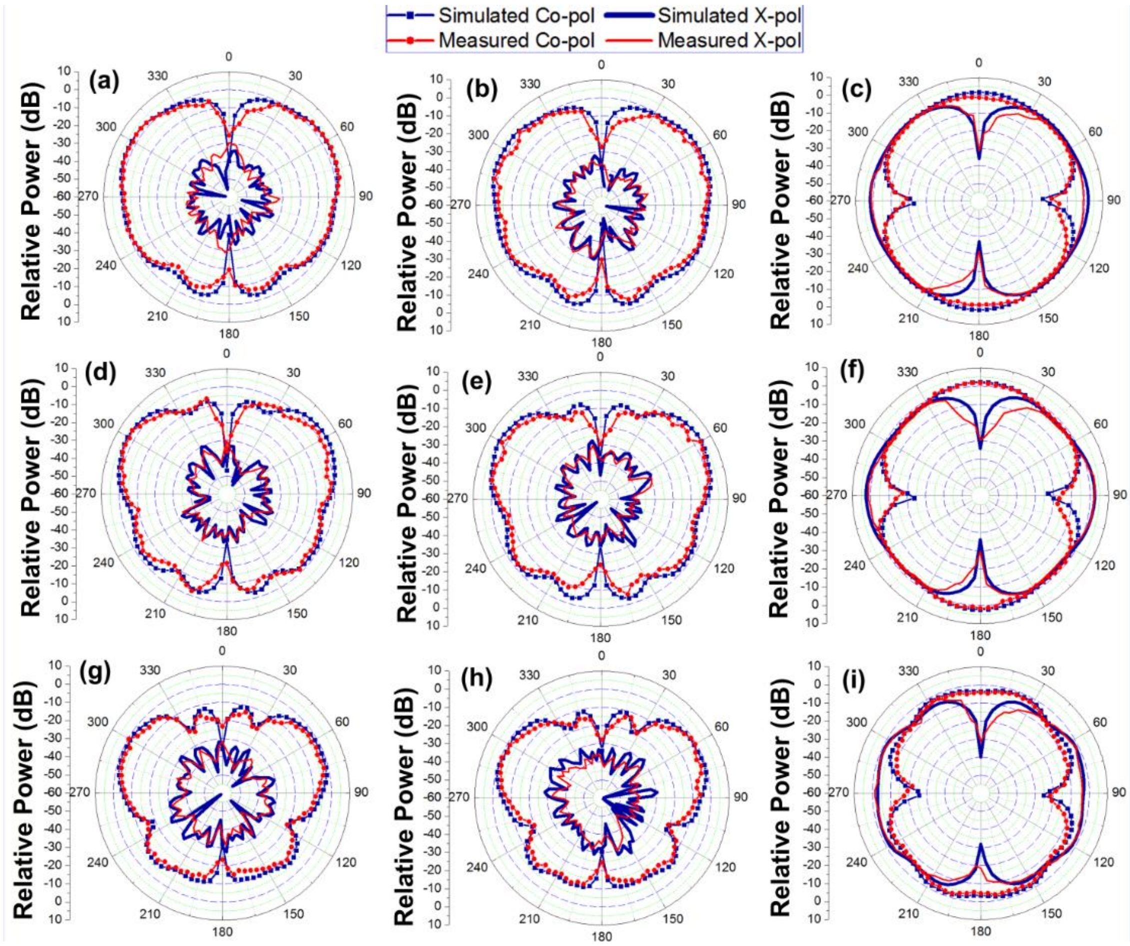

Figure 7.11 Radiation patterns of the proposed CDRA at (a) 9.50 GHz (in x-z plane); (b) 9.50 GHz (in y-z plane); (c) 9.50 GHz (in x-y plane); (d) 10.50 GHz (in x-z plane); (e) 10.50 GHz (in y-z plane); (f) 10.50 GHz (in x-y plane); (g) 11.25 GHz (in x-z plane); (h) 11.25 GHz (in y-z plane) and (i) 11.25 GHz (in x-y plane).

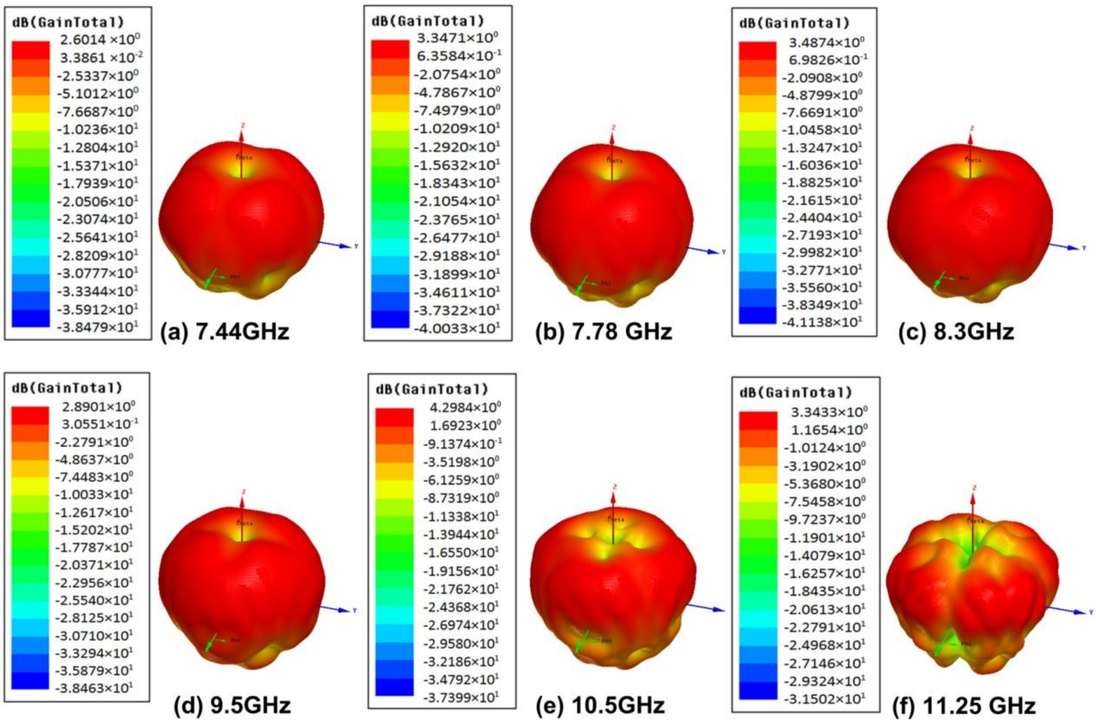

Figure 7.12 3D gain plots at different frequencies within the operating frequency range of the proposed CDRA.

Table 7.5 Comparison of the performance of the proposed antenna with other antennas reported in literature.

Parameters	**Reference [Guha et al. (2006b)]**	**Reference [Gangwar et al. (2017)]**	**Proposed CDRA**
Type of Feed for Excitation	Modified coaxial probe (coaxial probe surrounded by small dielectric rod)	Coaxial probe	Composite feed
Resonator Type	4-element Cylindrical resonator	4-element triangular resonator	Single element cylindrical resonator
Operating Frequency Range (GHz)	~3 – 4	4.7 – 6.8	7.03 – 11.98
Bandwidth (%)	~29	~37	~52
Gain (dB)	4.0	4.7	3.3
Fabrication Complexity	Complex	Moderate	Easy

The DRAs providing monopole radiation pattern previously reported in literature [Gangwar et al. (2017); Guha et al. (2006b)] have complex antenna structure. In the present work, emphasis is given on simpler DRA structure i.e. single segment cylindrical DRA which made its design less complex and its fabrication easier. In the proposed DRA, the antenna consists of single segment cylindrical DRA, which is excited by a novel composite feeding structure. The proposed feeding structure is a combination of a probe and XOR-shaped patch. The performance of the proposed antenna including the feed structure is compared with the antennas reported in literature (Table 7.5). It can be seen from Table 7.5 that the proposed antenna provides the widest bandwidth among the antennas studied, though resonant frequencies of antennas are different.

7.4 Summary

In the present chapter, BST-3B ceramic has been used for the design of SS-CDRA. Three different composite feed configurations have been proposed for the excitation of SS-CDRA with the objective of obtaining monopole like radiation patterns. The input characteristics and mode analysis for SS-CDRA have been performed for the three feed configurations (PPP, PSP and PXP). Further, both input and radiation characteristics of the proposed antenna, which is excited by PXP feed have been studied. The simulated and measured -10 dB reflection coefficient bandwidths for the proposed antenna have been determined to be 40.77 % (7.44 - 11.25 GHz) and 52.08 % (7.03 - 11.98 GHz), respectively. The E-field distributions show the generation of distorted $TM_{01\delta}$ mode in the proposed CDRA. The proposed antenna has provided monopole like radiation patterns. Simulated gain of 3.34 dB for the proposed antenna has been obtained at the resonant frequency of 7.78 GHz. The simulation and the experimental results of the proposed antenna have been found to be nearly in agreement with some deviation in the results for reflection coefficient-frequency characteristics which may be due to fabrication and measurement errors. The proposed antenna has also been found to provide the widest bandwidth when compared with other antennas producing monopole like radiation pattern reported in literature. The proposed CDRA may find potential application as an element in antenna array in radar and satellite communication. The benefits of the proposed antenna is in its simple design and simple feed layout for obtaining monopole like radiation characteristics. The composite feed employed here can be exploited for excitation of different DRAs using wide range of available dielectric materials, which can provide much flexibility to cover wide range of frequencies.